Draft version June 8, 2011
Preprint typeset using LaTeX style emulateapj v. 11/10/09



# THE EFFECTS OF X-RAY FEEDBACK FROM AGN ON HOST GALAXY EVOLUTION

D. Clay Hambrick and Jeremiah P. Ostriker
Princeton University Observatory, Princeton, NJ 08544

Thorsten Naab
Max-Planck-Insitut für Astrophysik, Karl-Schwarzschild-Str. 1, D-85741, Garching bei München, Germany

Peter H. Johansson
Finnish Centre for Astronomy with ESO, University of Turku, Väisäläntie 20, FI-21500 Piikkiö, Finland
Department of Physics, University of Helsinki, Gustaf Hällströmin katu 2a, FI-00014 Helsinki, Finland
Universitäts-Sternwarte München, Scheinerstr. 1, D-81679 München, Germany

*Draft version June 8, 2011*

## ABSTRACT

Hydrodynamic simulations of galaxies with active galactic nuclei (AGN) have typically employed feedback that is purely local: i.e., an injection of energy to the immediate neighborhood of the black hole. We perform GADGET-2 simulations of massive elliptical galaxies with an additional feedback component: an observationally calibrated X-ray radiation field which emanates from the black hole and heats gas out to large radii from the galaxy center. We find that including the heating and radiation pressure associated with this X-ray flux in our simulations enhances the effects which are commonly reported from AGN feedback. This new feedback model is twice as effective as traditional feedback at suppressing star formation, produces 3 times less star formation in the last 6 Gyr, and modestly lowers the final BH mass (30%). It is also significantly more effective than an X-ray background in reducing the number of satellite galaxies.

*Subject headings:* galaxies: elliptical and lenticular — galaxies: formation — methods: numerical

## 1. INTRODUCTION

It has been well established that massive galaxies typically contain massive black holes (BHs) at their centers, and it is widely believed that these black holes, while in their so-called "active galactic nuclei" (AGN) phases, can have profound influence on the galaxies which host them (see Ferrarese & Ford 2005 for a comprehensive observational review). This influence is inferred from, among other observations, the correlation between the BH mass and the bulge mass of the host galaxy, which was first noticed by Kormendy & Richstone (1995) and studied by Magorrian et al. (1998), and has since been repeatedly confirmed (Häring & Rix 2004), as has the somewhat tighter relation between the BH mass and the host bulge's velocity dispersion, discovered by Ferrarese & Merritt (2000) and Gebhardt et al. (2000). The inferred BH mass distribution has also been convincingly linked to the quasar luminosity function (Yu & Tremaine 2002).

Since the work of Silk & Rees (1998), the relationship between the AGN and host galaxy has generally been characterized as a process of feedback: the galaxy supplies gas to be accreted by the BH, which emits some fraction of the accreted mass as mechanical energy to the surroundings, some fraction via the broad-line winds, and some fraction as the radio jets. All these processes can heat the surrounding gas, and since gas which has been heated is less dense and thus accretes more slowly, the feedback process is described as "self-regulating" (i.e. a negative feedback loop).

Thus there are two modes by which AGN may give energy to their surroundings: the "mechanical" mode, where the AGN inflates local gas bubbles which expand through the inter-stellar and inter-galactic media (ISM/IGM) (Fabian et al. 2000; Churazov et al. 2002; Nulsen et al. 2005); and the "electromagnetic" mode, where photons from the AGN accretion region for which the neighboring gas has a low optical depth escape and directly interact with the rest of the ISM/IGM (Sazonov et al. 2005). Both of these modes may then interact with the surrounding galactic gas by either (or rather, both) of two mechanisms: energy-based (i.e. heating) (Silk & Rees 1998; Wyithe & Loeb 2003), or momentum-based (i.e. pressure) (Fabian, Celotti & Erlund 2006; DeBuhr, Quataert & Ma 2010). Ciotti & Ostriker (2007) have included both mechanisms in their ongoing work. Thus there are four conceptual components which feedback models may take into account: mechanical-energy (a.k.a. bubbles), mechanical-momentum (a.k.a. winds), electromagnetic-energy (a.k.a. radiative heating), and electromagnetic-momentum (a.k.a. radiation pressure). The relative importance of these components has been much debated among the authors just mentioned. A fifth component, the thin radio jets, emit comparable amounts of energy and momentum with the other modes, but these intense beams tend to drill through the galactic gas, depositing their energy in the IGM. This makes jets less relevant as a feedback method, unless they precess, or there is a relative

velocity between the AGN and its environment, in which case significant heating of galactic gas could occur (Sternberg & Soker 2009; Soker 2009).

There has naturally been much interest in reproducing the AGN feedback process via numerical simulations. Springel et al. (2005) were among the first to do so using a high-resolution 3D smoothed-particle hydrodynamics (SPH) code. They found that including an accreting BH particle which returns energy to the surrounding gas reduces the fraction of baryons which form stars, and at late times (for massive galaxies) expels most of the remaining gas from the host, creating the classic "red and dead" elliptical. Since then, many more SPH simulations have been done, exploring various aspects of AGN growth and feedback: Pelupessy et al. (2007), Khalatyan et al. (2008), Johansson, Burkert & Naab (2009), Johansson, Naab & Burkert (2009), and McCarthy et al. (2010), to name a few.

However, even though it has been shown that the emitted spectrum of the average AGN power $EF_E$ has a strong peak in the X-rays ($\sim$ 30 keV: Sazonov, Ostriker, & Sunyaev 2004), and moreover the ISM/IGM is known to be optically thin to hard X-rays in most cases (Morrison & McCammon 1983), all of the simulations just mentioned include only the mechanical-energy component of feedback. Some recent studies have included other components: Ostriker et al. (2010) examine the effect of mechanical-momentum feedback on AGN growth in 1 and 2D simulations and find that including this component reduces the final BH mass by a factor of 100; DeBuhr, Quataert & Ma (2010) insert mechanical-momentum feedback into a 3D SPH code (in fact the feedback was characterized as a radiation pressure, but only applied to the central 0.2 kpc of the galaxies, making it functionally mechanical) to examine its effects on the major mergers of disk galaxies, and found that with this component BHs self-regulate effectively during the mergers, but without driving large quantities of gas out of the galaxy altogether. Ciotti & Ostriker (2007), meanwhile, performed 1D simulations with the full electromagnetic mode, considering the heating and radiation pressure from the AGN radiation, but without the mechanical mode. They studied the potential cooling flows of "recycled" gas from dying massive stars, and found that the electromagnetic mode alone was sufficient to drive out half of the incoming gas, with the BH only accreting 1% of the total (the remainder forming a starburst). However, until now no 3D simulation has been performed with the electromagnetic mode included.

In Hambrick et al. (2009) (hereafter Paper I), we examined the effect of various ionizing radiation backgrounds on the properties of massive elliptical galaxies. In Hambrick et al. (2010) (hereafter Paper II), we examined the same backgrounds with respect to the small satellite galaxies of those massive ellipticals. Now we turn to a different source of ionizing radiation. It is the aim of this paper to present a first qualitative look at, and hint at quantitative results from, an AGN feedback model incorporating an X-ray electromagnetic mode.

The paper is organized as follows. In §2, we describe the numerical methods and parameters of our simulations, including the various AGN feedback models. In §3 we describe the results obtained from those simulations, in particular the effects of the different feedback models on the BHs themselves, on the gas and stars in the host galaxy and on the satellite galaxies. Section 4 is discussion and conclusion.

## 2. SIMULATIONS AND PARAMETERS

Our simulation code is GADGET-2, as in Paper II, with the only change being the addition of a black hole and associated feedback. We use the UV background of Faucher-Giguère et al. (2009) (which was designated as "FGUV" in Paper I and Paper II). The simulation includes SN thermal feedback but not winds or any stellar mass loss. It includes a simple prescription for metal-line cooling using cooling rates calculated by Cloudy (v07.02, last described in Ferland et al. 1998), which presumes photoionization and collisional equilibrium for the gas and metal atoms, and assumes 0.1 solar metallicity (note that our X-ray feedback code assumes solar metallicity, as discussed in §3.4). A self-consistent treatment of metallicity would increase the amount of cool gas available for accretion at later times and thus enhance the differences between our models. Our simulations do not include optical depth effects or radiative transfer, in particular the self-shielding of dense star-forming regions from the ionizing backgrounds, although those regions would be optically thin to X-rays regardless. As in Paper II, all simulations were performed with initially $100^3$ each of SPH (i.e. baryon) particles and DM particles, with a gravitational softening length of 0.25 kpc for the gas and star particles and twice that for the dark matter particles. Gas and star particles have masses in the range $4 - 7 \times 10^5 M_\odot$, depending on the size of the box; the assumed cosmology is $(\Omega_M, \Omega_\Lambda, \Omega_b/\Omega_M, \sigma_8, h) = (0.3, 0.7, 0.2, 0.86, 0.65)$ as in Paper II.

The BH feedback works as follows. At $z = 9$ a single seed BH particle of mass $1.5 \times 10^6 M_\odot$ is created at the point of minimum potential in the most massive progenitor halo. The seed mass is chosen to roughly follow the Magorrian relation for the galaxies at this redshift; the AGN behavior is not particularly sensitive to the seed mass (Hopkins et al. 2006). The BH grows at a modified Bondi-Hoyle-Littleton rate,

$$\dot{M}_{\rm BH} = \frac{4\pi\alpha_B (G M_{\rm BH})^2 \rho}{(v_{\rm BH}^2 + c_s^2)^{3/2}}, \quad (1)$$

where $M_{\rm BH}$ and $v_{\rm BH}$ are, respectively, the mass and speed (with respect to the surrounding gas) of the black hole, and $\rho$ and $c_s$ are the density and sound speed of the gas in the SPH kernel centered on the BH (Springel et al. 2005; Di Matteo, Springel & Hernquist 2005; Hopkins et al. 2006; Johansson, Naab & Burkert 2009). The free dimensionless parameter $\alpha_B$, which we choose to be 100, represents the fact that the gas density at the BH accretion radius is likely to be much higher than the average density in the local SPH kernel due to the limited resolution of the code (Hopkins et al. 2006; Booth & Schaye 2009). Future work could be done using the more realistic density-dependent accretion efficiency of Booth & Schaye (2009), which reduces to $\alpha = 1$ for large accretion radii. The Bondi-Hoyle accretion is capped at the Eddington rate, $\dot{M}_{\rm Edd} = 4\pi G m_P M_{\rm BH}/\epsilon_r c \sigma_T$. When the BH's notional mass as calculated from these accretion rates exceeds its true dy-

namical mass, the BH particle swallows nearby gas particles as needed to make up the difference. We enable artificial recentering of the BH particle on the potential minimum of the galaxy, since with our modest mass resolution dynamical friction is insufficient to keep the young BHs centered (though it is at late times, when the recentering has no effect).

We name our three feedback models "BH", "BHX" and "BHXRP". The "BH" model consists only of thermal energy deposited at each timestep in the SPH kernel centered on the black hole, in the amount of $\dot{E} = \epsilon_T \epsilon_r \dot{M}_{\rm BH} c^2$, where $\epsilon_r = 0.1$ is the overall radiative efficiency of the BH (Yu & Tremaine 2002), and $\epsilon_T$ the fraction of the radiation energy output which is assumed to be absorbed thermally by the local gas. Our choice of $\epsilon_T = 0.005$, together with our choice of $\alpha_B = 100$, is designed to produce a final ($z = 0$) BH mass roughly in line with the Magorrian relation for these galaxies. Note that our $\epsilon_T$ is 10 times smaller than than the value used in other GADGET-2-based simulations (e.g., Springel et al. 2005; Johansson, Naab & Burkert 2009), which is due to slightly different star-formation criteria than the generic GADGET-2 (a lower density threshold for star formation, a star-formation timescale which is shorter at low densities but constant at high densities and never shorter than the cooling time, and requiring the gas to fulfill a convergent flow criterion and the Bonnor-Ebert criterion to form stars), the upshot of which is that our stars form at somewhat lower gas densities, effectively lowering the BH accretion rate and thus its mass. Other simulations (e.g., Okamoto, Nemmen & Bower 2008; Ostriker et al. 2010) have used similarly low efficiencies around $\epsilon_T = 0.01$—on the other hand, the OverWhelmingly Large Simulations (OWLS) (Schaye et al. 2010), using a modified GADGET-3, find $\epsilon_T = 0.15$ to match the Magorrian relation, though also finding that the value should be reduced for lower resolution (Booth & Schaye 2009). Furthermore, observational evidence suggests a value $\epsilon_T \approx 0.015$ (Moe et al. 2009), although since we neglect important processes like stellar mass loss and chemical evolution, our value (and others') for $\epsilon_T$ is constrained far more by the simulation than by physics. At any rate, we are primarily interested in the relative differences between the models with and without radiative feedback, which should not be significantly affected by the exact star-formation prescription used. We call the mechanical-energy component "thermal" feedback for short to distinguish it from the X-ray feedback below. This energy component is of unspecified origin: if it is assumed to be the result of the broad-line wind, one should also include the momentum input (Ostriker et al. 2010), which has typically been neglected and which will not be included here.

The "BHX" model has the same feedback component just discussed, with the same assumed efficiencies, but adds another: the electromagnetic-energy component of X-ray radiation from the AGN. This radiation is emitted from the location of the BH particle with a luminosity of $L_X = \epsilon_X \epsilon_r \dot{M}_{\rm BH} c^2$, with a bolometric-to-X-ray conversion term $\epsilon_X$. This luminosity is converted to a flux at each gas particle simply by $F_X = L_X / 4\pi r^2$, with $r$ the distance of the particle from the BH, and the flux is converted to a heating rate for the gas using Eq. 36-43 in Ciotti & Ostriker (2007) (based on Sazonov, Ostriker, & Sunyaev 2005), taking only terms which are dependent on the ionization parameter $\xi \propto F_X$. These equations are parametrized in terms of bolometric flux, and implicitly assume $\epsilon_X \approx 0.04$ (as well as solar metallicity: see §3.4). We do not include radiative transfer/optical depth effects for this radiation (again, the ISM/IGM generally has a low optical depth to X-rays). Nor do we include a speed-of-light delay in propagation from the AGN across the box, but since our box's high-resolution region is only 2 Mpc in radius and we are most interested in the central 30 kpc, the effects of no delay should be small.

The "BHXRP" model adds a third component: electromagnetic-momentum, the radiation pressure from this X-ray flux, by applying to each gas particle a radial force away from the BH particle equal to the X-ray heating rate at that timestep divided by the speed of light $c$. We neglect the effect of dust, which dominates the opacity by several orders of magnitude at temperatures where it can exist ($T < 10^{3.5}$ K) (Semenov et al. 2003), making this component perhaps an underestimate (although as discussed in §3.3 below, our heating rate may be overestimated due to metallicity effects).

As an additional point of comparison, we run a set of simulations designated "BH+X". These have the same feedback mechanism as the regular BH runs, but also include an X-ray background field (which the others do not). This field is identical to the "FGUV+X" model in Paper II; see that paper for details. Briefly, the field peaks in strength around $z = 2$ and falls off sharply at earlier and later times, to roughly emulate the observed quasar background (i.e., the X-ray heat due to galaxies other than the one being simulated). This model allows us to differentiate the effects of X-rays originating in local AGN feedback from generic (spatially uniform) background radiation. We also compare to a model with no AGN activity whatever, "No BH".

We use three sets of initial conditions from Paper II that were designated galaxies/halos A, E, and M, and are so designated here as well. These are elliptical galaxies of virial mass $1 - 2 \times 10^{12}$ $M_\odot$. As will be discussed below, all the galaxies gave the same qualitative results. As in Naab et al. (2007), Johansson, Naab & Ostriker (2009) and Paper I, we choose galaxy A as our fiducial case, noting any differences from the others where relevant.

Throughout the paper, all distances are physical except where noted, with assumed $h = 0.65$ as in Paper I and Paper II.

## 3. RESULTS

### 3.1. *Evolution of the Black Hole Mass*

We first examine the effects of these various feedback mechanisms on the black hole itself. It is well-known that black holes are characterized only by mass, electric charge, and angular momentum (Bekenstein 1998), of which only the first is relevant here.

The top panel of Figure 1 shows the mass of the black hole for our four feedback models with galaxy A. Also shown is a model where the thermal feedback efficiency parameter $\epsilon_T$ has been increased by a factor of 2 to 0.01 (notated as "BH, 2xFB" in the figure). We see that although the additional feedback present in the BHX

and BHXRP models reduces the final black hole mass by 15% and 30% respectively, compared to the BH model, these changes are significantly less than the factor of 2 reduction we see in the model with increased thermal feedback—and another model with thermal feedback increased 10 times has a lower BH mass by a factor of 25. This is because the thermal feedback directly affects only the immediately neighboring gas particles, which are the same particles used to calculate the black hole's local density and thus its accretion rate, whereas the X-ray feedback affects all gas particles, thus making (as we will see) its effect on the host galaxy relatively stronger than its self-regulation effect, compared to thermal feedback.

On the other hand, the addition of an X-ray background in the BH+X model *increases* the final BH mass slightly (9%), due primarily to more gas being available in the merger event at $z = 0.7$. All the models except the enhanced thermal feedback model are consistent with the Magorrian relation for this galaxy, which predicts a black hole mass of $\sim 2 \times 10^8 M_\odot$, depending on model, using the fit of Häring & Rix (2004)—since the galaxies are ellipticals, we approximate "bulge mass" as the stellar mass within three stellar half-mass radii ($\sim 18$ kpc) of the galaxy center. We note here that if the electromagnetic feedback (heating and radiation pressure) is used in the absence of any mechanical feedback, the black hole becomes too large by three orders of magnitude: it seems that for our simulations the electromagnetic mode alone is insufficient for self-regulation. This differs from the result of Ciotti & Ostriker (2007), who found effective self-regulation using only electromagnetic feedback; we attribute the difference to their inclusion of dust opacity, which is certainly very important in AGN accretion regions (Scoville 2003), as well as their neglect of infalling satellite galaxies and IGM.

The lower panel of Figure 1 shows galaxy E, which is much the same as galaxy A, except for the major (1:1 mass ratio) merger event at $z \approx 1.5$ (10 Gyr ago), which drives a huge amount of gas to the BH and causes the mass to jump by a factor of $\sim 5$. Again in this case the BH+X model has the largest final mass (by ∼10%), thanks to the X-ray heating leaving more gas available to be accreted in the merger event. We also see that BHXRP accretes only half the gas of the other models at the moment of merger, making up the difference slowly over the next several Gyr; it seems that the radiation pressure is effective in blowing out the merging gas when X-ray heating and thermal feedback are not, consistent with DeBuhr, Quataert & Ma (2010). Otherwise, galaxies E and M are much the same as galaxy A, with BHX and BHXRP having lower black hole masses by roughly 15% and 30%.

Another factor which we do not model here is the creation and mergers of black holes in subhalos. For simplicity, we have created only one BH, in the largest halo at $z = 9$ (which remains the largest halo until the present). While we do not expect the lack to change our results qualitatively, including AGN in satellites would reduce gas mass and star formation in those systems, leaving less gas and stellar mass to be accreted by the central galaxy in minor and major mergers. The effect would be especially strong on systems like galaxies E, with its nearly 1:1 merger.

Figure 2 shows absolute accretion rates for the same

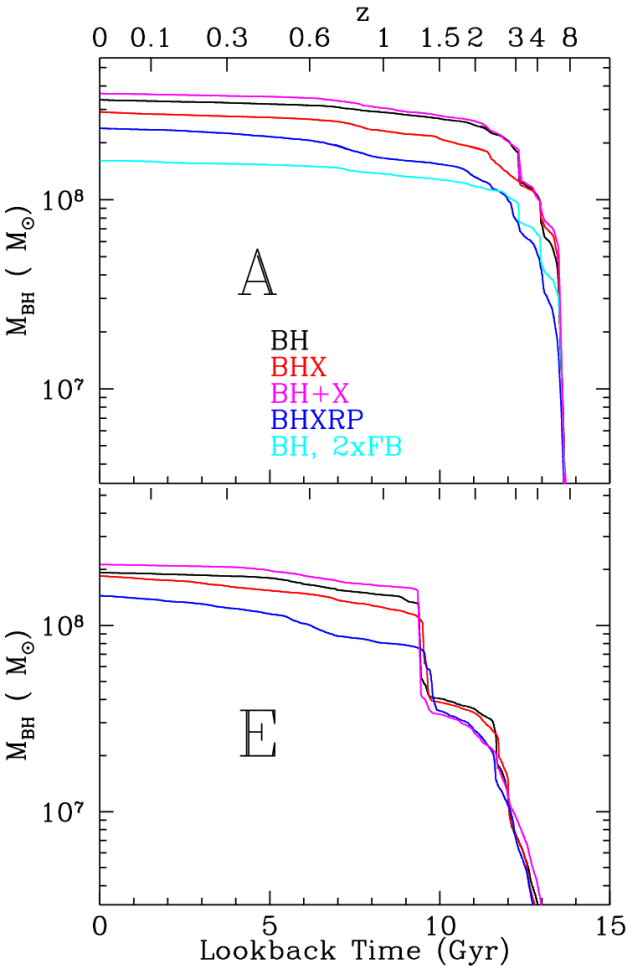


FIG. 1.— The mass of the central black hole for our various feedback models, in galaxy A (top) and galaxy E (bottom). Adding the X-ray feedback and radiation pressure decreases the final BH mass by 30%, while increasing the thermal feedback by a factor of 2 reduces the final mass by a factor of 2.

models with galaxy A. The rates are smoothed over 160 Myr for clarity; the BH accretion shows high variability over timescales as short as a few timesteps ($\sim$ 100 kyr). For the models with lower thermal feedback, the rate peaks near $1 M_\odot$/yr around $4 \gtrsim z \gtrsim 3$, and slowly declines thereafter to a final value of $\sim 0.003 M_\odot$/yr, except for the peak around $z \approx 0.7$, which corresponds to a moderate (6.5 : 1) merger event for Galaxy A. Of interest is the suppression of the accretion spike at $z = 3$ for the BHX model, and all three accretion spikes (at $z = 6, 4, 3$) by BHXRP: we see that these feedback modes are effective at self-regulation for very high accretion rates. Also of note is that for 4 Gyr after the merger BHXRP has more accretion than the other models by a factor of 2 (which will be significant in §3.3).

In the following subsections we disregard the model with enhanced thermal feedback; in all cases its effects are the same or weaker than the plain BH model.

### 3.2. *Impact on Gas*

We now turn to the effects of the various BH models on the host galaxy. We expect our X-ray feedback to be quite effective at heating gas, and indeed it is. Figure 3 shows the temperature distribution of all gas in

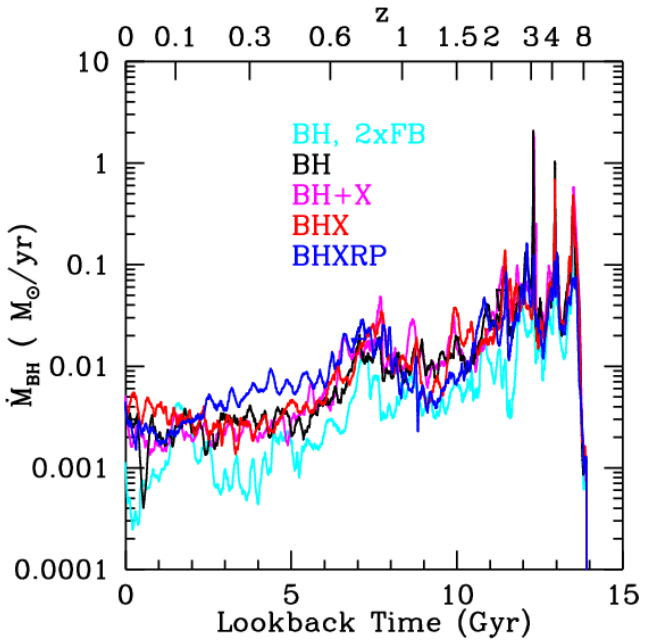


FIG. 2.— The accretion rate for galaxy A in $M_\odot$/yr with the different feedback models. Accretion peaks at $z = 3$ and again with the major merger at $z = 0.7$, after which BHXRP has a sustained period of higher accretion. The X-ray luminosity is proportional to the accretion rate ($L_X = \epsilon_X \epsilon_r \dot{M}_{\rm BH} c^2$), with $1 M_\odot$/yr corresponding to $2 \times 10^{44}$ erg/s. The sharp spikes at $7 > z > 3$ correspond to bursts of Eddington-limited accretion.

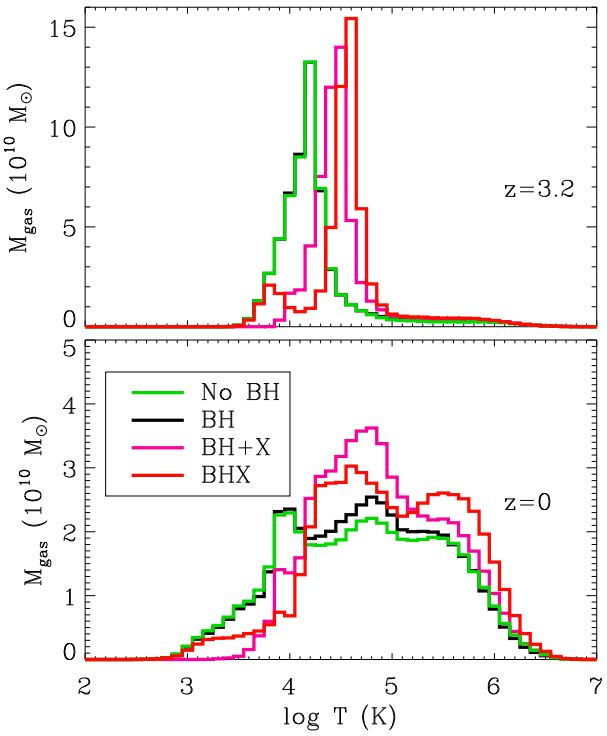


FIG. 3.— Temperature distribution of all gas in the box for halo A at $z = 3.2$ (top panel) and $z = 0$ (bottom panel). BHXRP, not shown, is nearly identical to BHX; No BH and BH are nearly identical in the top panel. The BHX and BHXRP models have a 10% higher mean temperature than the BH+X model at $z = 3.2$, and 25% higher at $z = 0$.

the halo A box at $z = 3.2$ (during the epoch of peak star formation) and the present. At $z = 3.2$, the No BH model has the coldest gas, with a mean temperature of $6.4 \times 10^4$ K. Adding BH thermal feedback heats the gas 11% to $7.1 \times 10^4$ K, and adding an X-ray background heats it 24% more to $8.8 \times 10^4$ K. However the two BHX models are more effective by another 9%, giving a mean gas temperature of roughly $9.6 \times 10^4$ K. At $z = 0$, the effect of feedback X-rays is more pronounced compared to a background: BHX and BHXRP, at a mean temperature of $3 \times 10^5$ K, are 25% hotter than BH+X, which in turn is only 14% hotter than BH and No BH.

Figure 4 is the same as Figure 3, except that it shows only virialized gas: gas with a density more than 200 times the mean baryon density. Here the effect of the AGN feedback X-rays is more pronounced, as we would expect, since most of the virialized gas is near the central galaxy, where the AGN X-rays are strongest. At $z = 3.2$, the three models without X-ray feedback are all within 10% of each other in mean temperature at roughly $9 \times 10^4$ K, while BHX and BHXRP have mean temperatures of $1.6 \times 10^5$ K and $1.3 \times 10^5$ K respectively, 40-80% higher than the other models. At $z = 0$ the picture is even more extreme. BHX and BHXRP have $2.4 \times 10^{10} M_\odot$ and $3.0 \times 10^{10} M_\odot$, respectively, of virial X-ray gas $> 10^{5.5}$ K, more than 4 times the amount that BH+X has, and 6 times the amount of the other models. Unlike the Warm-Hot Intergalactic Medium (WHIM), which is usually defined as $\rho < 100 \bar{\rho}_b$ (Smith et al. 2010), this gas is dense enough to emit significant soft X-rays.

We estimate the (Bremsstrahlung) X-ray luminosities of the various models via

$$L_X \propto \int \rho^2 \sqrt{T} dV$$

(Evrard 1990) for gas above $2 \times 10^6$ K over the virial volume (a 500 kpc radius), and find that all models have $\log L_X \approx 38 - 39.5$, consistent with the gas luminosities found by Boroson, Kim & Fabbiano (2011) for 30 early-type galaxies of similar size. The differences between BH models is modest: averaged over the three ICs, the BH+X, BHX and BHXRP models have increased luminosity by factors of 1.6, 2, and 3, respectively, compared with the models without X-rays. Adding BH feedback also increases the X-ray effective radius: only 33% of the total X-ray luminosity for No BH comes from outside the central 10 kpc, while 63% does for BH and BH+X, 68% for BHXRP and 73% for BHX (again averaging the 3 ICs).

### 3.3. *Impact on Stellar Mass*

We naturally expect the hotter gas produced by the AGN X-ray feedback to reduce the production of stars. The upper panel of Figure 5 shows the star-formation rate (SFR) over time for galaxy A, out to a radius of 30 kpc. We see only modest differences in the initial star-formation peak (see below), but BH+X and BHXRP are both effective at suppressing late star formation: BHXRP has a lower SFR than the other models by 0.5 dex for the the last 6 Gyr ($z < 0.6$), while BH+X suppresses the SFR by 0.8 dex for the last 1.5 Gyr ($z < 0.1$). BHXRP forms $3.4 \times 10^9$ $M_\odot$ of stars in the host galaxy after $z = 0.5$, and BH+X $3.6 \times 10^9$ $M_\odot$, which is less than half of the roughly $7.2 \times 10^9$ $M_\odot$ formed by the other models. The BH+X result is interesting in the con-

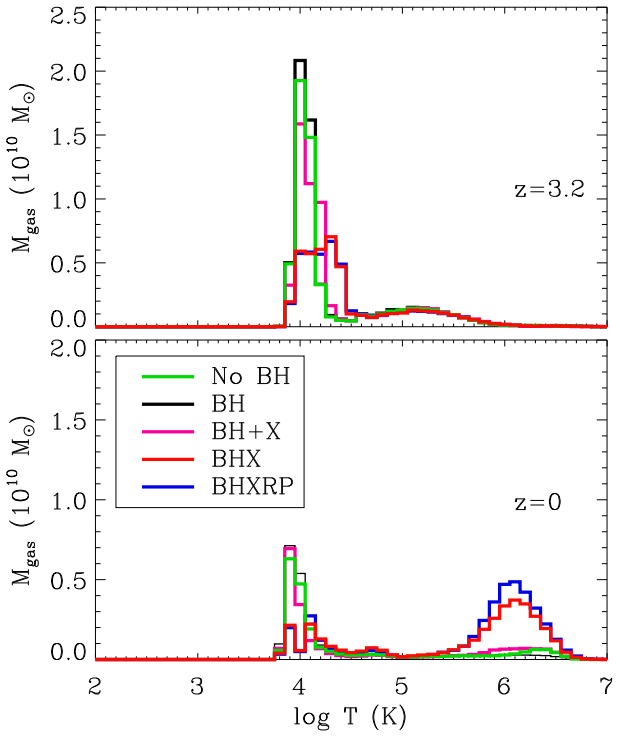


FIG. 4.— Temperature distribution of virialized gas ($\rho > 200\bar{\rho}_b$) in the whole box for halo A at $z = 3.2$ (top panel) and $z = 0$ (bottom panel). At $z = 3.2$, the X-ray feedback models have a higher mean temperature than the other models by a factor of 1.5, and at $z = 0$ they are hotter by a factor of 2.

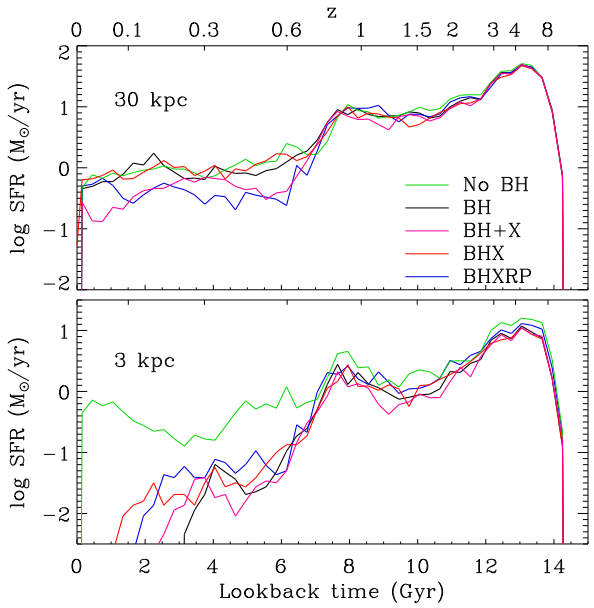


FIG. 5.— Log of the star-formation rate over time for galaxy A with the various feedback models, considering stars within 30 kpc (upper panel) and 3 kpc (lower panel) of the galaxy center at $z = 0$. Where the curves drop off the bottom of the plot they go all the way to zero. BHXRP and BH+X are both effective at suppressing late star formation for the whole galaxy, while in the center adding X-ray feedback actually keeps star formation going longer.

text of Paper I, where the X-ray background produced a strong burst of late star-formation, as gas that had been kept hot through the X-ray background peak at $z \approx 2$ finally cools and flows to the center of the galaxy to form stars (the so-called "cooling flow"). Here, a cooling flow seems to be forming around redshift of 0.3 (see the lower panel of Figure 5), but the AGN effectively shuts it off. The effect with BHXRP, meanwhile, is clearly related to its enhanced accretion rate after the merger event: we see from Figure 1 that BHXRP accretes less gas during a major merger, leaving a residual which forms a few central stars (see below), but more importantly powers extra feedback for the next several Gyr, suppressing star formation at larger radii.

The lower panel of Figure 5 shows the SFR for galaxy A out to a radius of only 3 kpc (the 3D stellar half-mass radius for the galaxy is the range $5-8$ kpc). The results here are somewhat different: while all the models with BHs have no star formation at the present, BHX and BHXRP have nonzero star formation until roughly 1.5 Gyr ago, compared to 3 Gyr for the plain BH model (and 2.5 Gyr for BH+X). In terms of mass, BHX forms $1.7 \times 10^8$ $M_\odot$ in the central 3 kpc after $z = 0.5$, BHXRP $2.8 \times 10^8$ $M_\odot$ (the residual from the merger just discussed), which is $2-3$ times more than the $1 \times 10^8$ $M_\odot$ formed by BH and BH+X, but still less than a tenth of the No BH model ($3.1 \times 10^9$ $M_\odot$). This is an expected result: as in Paper I, when X-ray heating is present, more gas is available at moderate and low redshift ($z < 2$) to be drawn to the galaxy's center in major mergers and in cooling flows, and the AGN feedback, while eventually preventing most of this gas from forming stars, cannot do so immediately.

TABLE 1
STELLAR MASS RESULTS

| IC | Feedback | $M_R$(5kpc) | $M_R$(30kpc) | $M_R$(2Mpc) | $\epsilon_\star$ |
|---|---|---|---|---|---|
| A | No BH | 9.58 | 19.43 | 50.35 | 0.543 |
| A | BH | 6.27 | 18.12 | 48.09 | 0.525 |
| A | BH+X | 5.85 | 16.62 | 42.70 | 0.476 |
| A | BHX | 6.46 | 17.05 | 42.99 | 0.472 |
| A | BHXRP | 7.70 | 17.76 | 43.90 | 0.481 |
| E | No BH | 8.59 | 15.53 | 38.61 | 0.580 |
| E | BH | 7.45 | 14.70 | 37.98 | 0.534 |
| E | BH+X | 7.41 | 14.50 | 34.39 | 0.536 |
| E | BHX | 8.16 | 14.48 | 34.00 | 0.521 |
| E | BHXRP | 7.48 | 14.64 | 33.29 | 0.514 |
| M | No BH | 6.64 | 11.91 | 25.72 | 0.631 |
| M | BH | 5.42 | 11.91 | 23.64 | 0.594 |
| M | BH+X | 4.62 | 10.02 | 20.64 | 0.561 |
| M | BHX | 5.34 | 10.77 | 20.06 | 0.596 |
| M | BHXRP | 5.51 | 10.22 | 20.21 | 0.553 |

NOTE. — Results are for stars within the specified radius of the principal halo at $z = 0$. Masses are $10^{10} M_\odot$. The last column is the ratio of stellar to total (implied) baryonic mass for the central galaxy. Adding X-rays significantly decreases the total stellar mass and galactic stellar mass, while the BHXRP model actually increases the mass in the center of the host galaxy, and $\epsilon_\star$, in 2 of 3 cases.

Table 1 shows the stellar mass of the host galaxy for the various models and ICs at three radii: 5 kpc, 30 kpc and 2 Mpc (which is essentially the whole box). The total star formation in the box (column 5) is suppressed slightly (5%) by the presence of the AGN, but the X-rays, whether from the AGN or the background, reduce

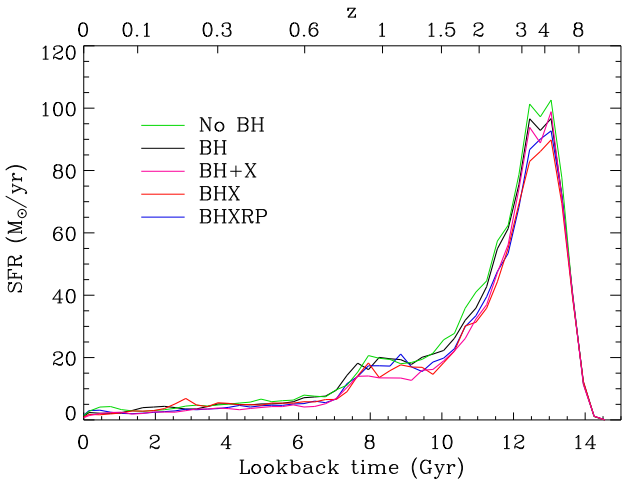


FIG. 6.— Star-formation rate over time for the various feedback models, considering stars within the whole box (2 Mpc radius) of galaxy A (galaxies E and M are similar). BHX and BHXRP effectively suppress the SFR peak at $4 > z > 3$, while the X-ray background reduces star-formation at $1.5 > z > 1$.

the total stellar mass by 15%, three times as much. However, the background X-rays and the feedback X-rays cause their suppression differently: as we see in Figure 6, which shows the star-formation history of the entire box for the halo A runs, the two models with X-ray feedback suppress the star-formation peak at $4 > z > 3$, while BH+X is most effective at a somewhat lower redshift, $1.5 > z > 1$. This clearly reflects the relative timing of the X-ray flux between the feedback and background sources, since the X-ray background peaks in intensity at $z \approx 2$, while the X-rays from feedback peak when the BH accretion rate does, at $4 > z > 3$. Thus BHX can have a strong effect on the SFR peak—recall that in Figures 3 & 4 we saw that BHX has hotter gas than BH+X at $z = 3.2$—while later when the local AGN is less active, the X-ray background is relatively more effective. This difference in timing also produces a substantial effect on how the stellar mass is distributed, as we will see in the next subsection.

The stellar mass in the central galaxy (column 4 of Table 1) is more or less as one would expect: thermal feedback and X-rays each reduce the stellar mass by a modest amount ($\sim$10%). To present the same results in a different way, the last column of Table 1 shows the baryon-conversion efficiency for the host galaxy, in this case identified using the Amiga Halo Finder (AHF: Knollmann & Knebe 2009). The value $\epsilon_\star$ is defined as it was in §4.2 of Paper II, $\epsilon_\star \equiv M_\star/M_{\rm Halo}(\Omega_M/\Omega_b) = 5M_\star/M_{\rm Halo}$ for our cosmology, where $M_\star$ is the halo's mass in star particles within 0.1 virial radii of the center and $M_{\rm Halo}$ its total virial mass. As discussed in Paper II, the absolute efficiencies for our models are all significantly higher than the value derived from SDSS by Guo et al. (2010), $\sim$0.2, but we are interested in the differences between the models. The two models with only thermal feedback reduce the efficiency by 0.035 from the No BH case, while adding the X-ray feedback (or an X-ray background in 2 of 3 cases) reduces it by an additional 0.035. So our most effective model, BHXRP, reduces the baryon-conversion efficiency by 7% from No BH. This is only one fifth of the reduction which would be necessary to bring our simulations in line with Guo et al. (2010), but still a significant difference.

We find more unexpected effects in column 3 of Table 1, which gives the stellar masses for the central 5 kpc of the galaxy. For galaxy A, the BHXRP model has almost 20% more mass than the other AGN models (though still 20% less than the No BH case), and 4% more than BHX at the 5 kpc radius. Once again this turns out to be associated with the SFR peak (though a small part comes from the extra late star formation discussed above): we see in the upper panel of Figure 7 that BHXRP has significantly more star formation in the peak at $z \approx 4$. This is clearly related to what we saw in the previous subsection: since BHXRP's feedback is more effective at self regulation, it accretes less strongly at $z \approx 4$ and thus provides less heating to the surrounding gas, which can thus form more stars. I.e., since the gas is pushed out by the feedback instead of merely being heated, the ability of the gas to form stars is less impaired even as the BH reduces its own growth rate. This effect is not robust, however: in the smaller galaxy M BHXRP has only barely more central mass than the other BH models, and in galaxy E it is BHX which has the most. But in this case BHX has slightly less stellar mass within 30 kpc than BHXRP, so it is only the central concentration which has been enhanced. This is related to the major merger event which galaxy E experiences: the extra residual gas from the early X-ray heating compared the no-BHX models means more gas is driven to the center to form stars during and after the merger, which we can seen in the lower panel of Figure 7. Meanwhile the radiation pressure in BHXRP forces this gas back out, as suggested by Figure 1, so it forms stars at larger radii, in agreement with DeBuhr, Quataert & Ma (2010).

Figure 8 gives the radial mass distributions for galaxy A in the form of circular speeds. As we would expect from column 3 of Table 1, No BH has the highest peak speed and the steepest inner slope, with BH, BH+X and BHX lower by about 25% in peak stellar circular speed and BHXRP in between. We can also parametrize the mass distribution with a "Faber-Jackson" statistic, $\sigma^4/M_\star$, where $\sigma$ is the (3D) stellar velocity dispersion and $M_\star$ the stellar mass within some radius of the galaxy center (we choose 30 kpc). This statistic should be roughly constant for various elliptical galaxies (Faber & Jackson 1976), but we find a variation of 40% between models, with the No BH case being the highest at 0.065 $(\mathrm{km/s})^4/\mathrm{M}_\odot$ (corresponding to the most central concentration), BH+X and BHX the lowest at 0.047 $(\mathrm{km/s})^4/\mathrm{M}_\odot$, and the other models intermediate. Similar results are obtained with the other galaxies. All these values are lower by a factor of $\sim$3 than the observational value of 0.22 $(\mathrm{km/s})^4/\mathrm{M}_\odot$ derived from the $M_\star - \sigma$ relation compiled by Robertson et al. (2006), but within the intrinsic scatter (and quite similar to those authors' simulation results for $z = 0$).

### 3.4. *Effects beyond the host*

Inspired by the differences between BH+X and BHX in their overall star-formation histories (Figure 6), we revisit the topic of Paper II and examine the low-mass slope of the galaxy mass spectrum, as parametrized by the $\alpha$ of Schechter (1976), which we will call $\alpha_S$ to dis-

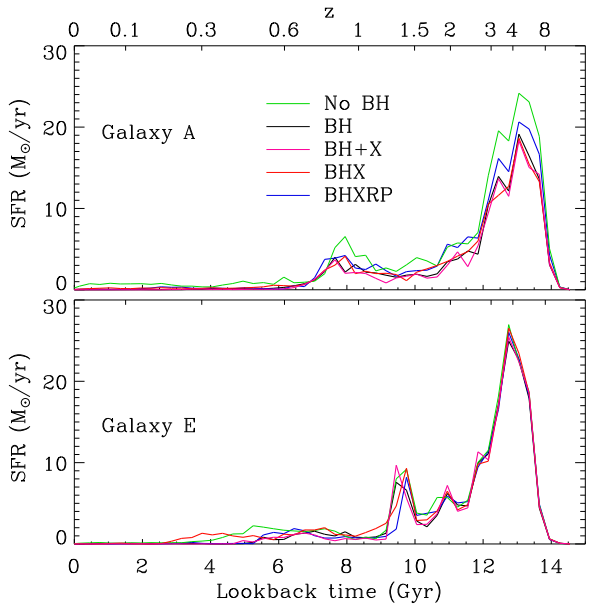


FIG. 7.— Star-formation rate over time for the various feedback models, considering stars within 5 kpc of the galaxy center for galaxy A (top panel) and galaxy E (bottom panel) at $z = 0$. In galaxy A, BHXRP allows significantly more central star formation than the other BH models, while the major merger in galaxy E causes more star formation for BHX.

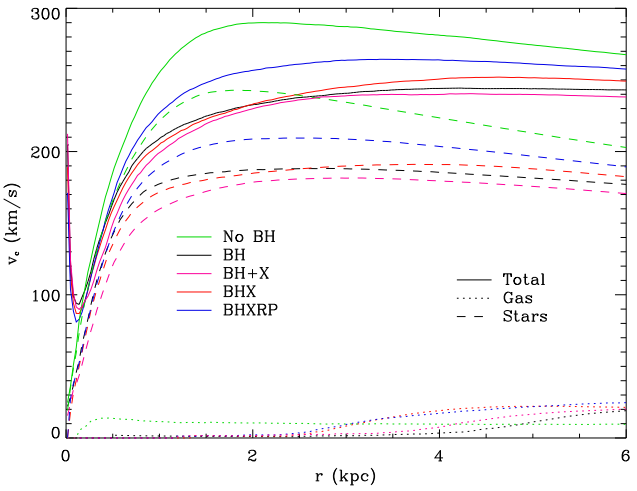


FIG. 8.— Circular speed for stars (dashed line), gas (dotted line), and total (solid line; also includes dark matter and the BH particle), for galaxy A with the various feedback models, $z = 0$. The upturn for the total circular speed curves in the innermost 200 pc is due to the mass of the BH particle itself (hence it is not present in the No BH model). Adding BH feedback lowers the peak value and flattens the inner slope, although adding radiation pressure reverses those effects somewhat for this galaxy. All BH models remove residual gas from the inner 2 kpc.

tinguish it from the Bondi accretion parameter $\alpha_B$. As in Paper II $\alpha_S$ is defined for our purposes by $n(M)dM \propto (M/M_*)^{\alpha_S} e^{-M/M_*} dM$. The results are given in Table 2: while the No BH and BH models agree within error with the values corresponding to their background from Paper II (and BH+X has a modestly steeper slope likely related to the suppression of cooling flows), the BHX and BHXRP models indeed have an extreme effect on $\alpha_S$, flattening it well beyond the observed value of $\sim -1$ to $-0.44$ and $-0.55$, respectively. In Paper II we found that $\alpha$ increases as any heating is added: from $-1.6$ with no heating, to $-1.3$ with a UV background, to $-1.0$ with UV and SN feedback, to $-0.75$ with UV, feedback and an X-ray background. As mentioned above, the timing of the X-rays seems to explain the difference between BH+X and BHX, since the BHX X-rays peak just before the epoch of primary star formation in low-mass galaxies (found in Paper II to be $3 \gtrsim z \gtrsim 2$), while the X-ray background peaks toward the end of it, and doesn't significantly suppress star formation until $z \approx 1.5$.

TABLE 2
SCHECHTER $\alpha$ VALUES AND MAXIMUM "BARREN" HALO MASSES WITH VARIOUS BACKGROUNDS

| Name | $\alpha_\star$ | $\log f M_{\rm crit}$ |
|---|---|---|
| No BH | $-1.09 \pm 0.04$ | $8.67 \pm 0.07$ |
| BH | $-0.96 \pm 0.14$ | $8.65 \pm 0.01$ |
| BH+X | $-0.84 \pm 0.12$ | $8.76 \pm 0.09$ |
| BHX | $-0.44 \pm 0.13$ | $8.95 \pm 0.08$ |
| BHXRP | $-0.55 \pm 0.08$ | $8.88 \pm 0.03$ |

NOTE. — The Schechter-$\alpha$ values for the star particles, maximum "barren" halo masses, and overall baryon-conversion efficiency with various ionizing background and AGN feedback models. X-ray feedback from the AGN greatly suppresses small stellar systems.

This result suggests that our X-ray feedback might be too strong: in fact, our formula converting X-ray flux to heating rate has a term (representing the photoionization heating and line and recombination cooling, Eq. A35 in Sazonov, Ostriker, & Sunyaev 2005) which is linear in $Z/Z_\odot$—i.e. the metallicity as a fraction of solar—where solar metallicity is assumed (Sergey Sazonov, private communication). Thus, since the metallicity of the ISM could be $0.1 Z_\odot$ at early times, our heating rate could be too high by that factor. Moreover, the work of Hui & Haiman (2003) suggests that after reionization the equilibrium temperature of the IGM is roughly independent of the intensity of the radiation field, depending only on its spectrum, so our $r^{-2}$ attenuation factor may be less significant than we would naïvely think.

The results for $f M_{\rm crit}$ are more modest. The quantity $f M_{\rm crit}$ is defined in Paper II: in short, it represents the largest halo mass at which halos have an average star:DM mass ratio of less than half the global value (0.08). ($M_{\rm crit}$ is the theoretically-calculated virial mass whose escape velocity is equal to the sound speed of its gas at the epoch when it should be forming stars; the effective correction factor $f \approx 0.75$.) Here again, No BH, BH, and BH+X agree well with the values that Paper II gives from their ionizing background models. The X-ray background models have somewhat higher values, as we would expect from their flatter low-mass slopes.

## 4. DISCUSSION & CONCLUSIONS

The effects of X-ray feedback from AGN are manifold. We find that X-ray heating and radiation pressure are only moderately effective at self-regulation: they reduce

the black hole's mass far less than increasing the thermal feedback efficiency does, primarily by suppressing bursts of Eddington-limited accretion at early times. The model with radiation pressure also accretes significantly less gas at the time of a major merger, instead accreting it more smoothly over the following several Gyr. The X-ray feedback produces a significant reduction in the host galaxy's baryon-conversion efficiency compared to a traditional feedback model, but only slightly more than a model with traditional feedback and an X-ray background. We note however that our baryon-conversion efficiency remains well above the observationally-derived value; though this problem is hardly unique to the present work it remains troublesome. On the other hand, less star formation would leave more gas available for AGN accretion, which would likely enhance the relative effect of electromagnetic feedback.

The enhanced accretion and associated feedback in the radiation-pressure model can also sustain a half-decade reduction in the star-formation rate of the host galaxy for several Gyr after a major merger event, although the gas required for this extra feedback leads to more star formation in the central regions, which in turn can lead to enhanced central concentration. The AGN X-ray feedback also produces a significant mass of virialized, soft-X-ray-emitting gas at the present, which the X-ray background does not have (when ordinary AGN thermal feedback is present; in Paper I we found a significant mass in hot, dense gas for a model with X-ray background but no AGN feedback), which increases both the X-ray luminosity and the X-ray half-light radius. In a serendipitous final result, we find that this X-ray feedback is also much more effective than an X-ray background in suppressing small galaxies and thus flattening the low-mass slope of the galaxy mass spectrum, due to its feedback's local origin making it effective at heating gas some $2-3$ Gyr earlier than the background.

Since AGN are known to emit X-rays through their host galaxies, we view this study as a vital first step toward a more complete model of AGN feedback. Moreover, since the X-ray luminosity of AGN is relatively well constrained by observations (though not without intrinsic scatter), there is little need for a new free parameter to join the current $\alpha_B$ and $\epsilon_T$ (modulo the effects of metallicity and dust). Thus we hope that this "new" feedback mode will be employed in future SPH simulations of AGN, since it is both undeniably present and, as we have shown, substantial in effect.

JPO was supported by NSF grant AST 07-07505 and NASA grant NNX08AH31G. TN and PHJ acknowledge support by the DFG cluster of excellence 'Origin and Structure of the Universe'.

REFERENCES

Bekenstein, J.D., arXiv:gr-qc/9808028
Booth, C.M., & Schaye, J., 2009, MNRAS, 398, 53
Boroson, B., Kim, D.-W., Fabbiano, G., 2011, ApJ, 729, 12
Churazov, E., Sunyaev, R., Forman, W., Böhringer, H., 2002, MNRAS, 332, 729
Ciotti, L. & Ostriker, J.P., 2007, ApJ, 665, 1038
DeBuhr, J., Quataert, E., & Ma, C.-P., 2010, arXiv:1006.3312
Di Matteo, T., Springel, V., & Hernquist, L., 2005, Nature, 433, 604
Evrard, A.E., 1990, ApJ, 363, 349
Faber, S.M., & Jackson, R.E., 1976, ApJ, 204, 668
Fabian, A.C., Celotti, A., & Erlund, M.C., 2006, MNRAS, 373, 16
Fabian, A.C. et al., 2000, MNRAS, 318, 65
Faucher-Giguère, C.-A., Lidz, A., Zaldarriaga, M., Hernquist, L., 2009, arXiv:0901.4554
Ferland, G. J., Korista, K.T., Verner, D.A., Ferguson, J.W., Kingdon, J.B., & Verner, E.M., 1998, PASP, 110, 761
Ferrarese, L. & Ford, H., 2005, Space Sci. Rev., 116, 523
Ferrarese, F., & Merritt, D., ApJ, 539, 9
Gebhardt, K. et al., 2000, ApJ, 539, 13
Guo, Q., White, S., Li, C., & Boylan-Kolchin, M., 2010, MNRAS, 404, 1111
Häring, N. & Rix, H., 2004, ApJ, 604, 89
Hambrick, D.C., Ostriker, J.P., Naab, T., & Johansson, P.H., 2009, ApJ, 705, 1566
Hambrick, D.C., Ostriker, J.P., Naab, T., & Johansson, P.H., 2009, arXiv:1009.6005
Hopkins, P.F., Hernquist, L., Cox, T.J., Robertson, B., Di Matteo, T., & Springel, V., 2006, ApJ, 639, 700
Hui, L., & Haiman, Z., 2003, ApJ, 596, 9
Johansson, P.H., Burkert, A., & Naab, T., 2009, ApJ, 707, 184
Johansson, P.H., Naab, T., & Burkert, A., 2009, ApJ, 690, 802
Johansson, P.H., Naab, T., & Ostriker, J.P., 2009, ApJ, 697, 38
Khalatyan, A. et al., 2008, MNRAS, 387, 13
Knollmann, S.R. & Knebe, A., 2009, ApJS, 182, 608
Kormendy, J. & Richstone, D., 1995, ARA&A, 33, 581
Magorrian, J. et al., 1998, ApJ, 115, 2285
McCarthy, I.G. et al., 2010, MNRAS, 406, 822
Moe, M., Arav, N., Bautista, M.A., & Korista, K.T., 2009, ApJ, 706, 525
Morrison, R. & McCammon, D., 1983, ApJ, 270, 119
Naab, T., Johansson, P.H., Ostriker, J.P., & Efstathiou, G. 2007, ApJ, 658, 710
Nulsen, P.E.J., Hambrick, D.C., McNamara, B.R., Rafferty, D., Birzan, L., Wise, M.W., & David, L.P., 2005, ApJ, 625, 9
Okamoto, T., Nemmen, R.S., & Bower, R.G., 2008, MNRAS, 385, 161
Ostriker, J.P., Choi, E., Ciotti, L., Novak, G.S., & Proga, D., 2010, ApJ, 722, 642
Pelupessy ,F.I., Di Matteo, T., & Ciardi, B., 2007, ApJ, 665, 107
Robertson, B., Hernquist, L., Cox, T.J., Di Matteo, T., Hopkins, P.F., Martini, P., & Springel, V., 2006, ApJ, 641, 90
Sazonov, S.Yu., Ostriker, J.P., Ciotti, L., Sunyaev, R.A., 2005 MNRAS, 358, 168
Sazonov, S.Yu., Ostriker, J.P., & Sunyaev, R.A. 2004 MNRAS, 347, 144
Sazonov, S.Yu., Ostriker, J.P., Ciotti, L., & Sunyaev, R.A. 2005, MNRAS, 358, 168
Scoville, N., 2003, J. Kor. Ast. Soc., 36, 167
Schaye, J., et al., 2010, MNRAS, 402, 1536
Silk, J. & Rees, M., 1998, A&A, 331, 1
Springel, V., Di Matteo, T., & Hernquist, L., 2005, MNRAS, 361, 776
Schechter, P., 1976, ApJ, 203, 297
Semenov, D., Henning, Th., Helling, Ch., Ilgner, M., & Sedlmayr, E., 2003, A&A, 410, 611
Smith, B.D., Hallman, E.J., Shull, J.M., & O'Shea, B.W., 2010, arXiv:1009.0261
Soker, N., 2009, MNRAS, 398, 41
Sternberg, A., & Soker, N., 2009, MNRAS, 398, 422
Wyithe, J.S. & Loeb, A., 2003, ApJ, 595, 614
Yu, Q., & Tremaine, S., 2002, MNRAS, 335, 965